Available online at www.sciencedirect.com

SciVerse ScienceDirect

Procedia Engineering 00 (2015) 000–000

Procedia Engineering

www.elsevier.com/locate/procedia

7th International Conference on Fluid Mechanics, ICFM7

Measuring large scale flow structures behind a bluff body using a hot-wire rake

Nan Gao[1,*], Yaqing Li[1], Honglei Bai[b]

[a]*School of Aeronautics and Astronautics, Dalian University of Technology, Dalian, China*
[b]*Department of Mechanical Engineering, University of Melbourne, Melbourne, Australia*

Abstract

Wake behind a D-shaped bluff body were studied using experimental method. The forcing amplitude was $C_\mu = 0.1\%$. A rake of 14 hot-wire probes were used to measure the instantaneous velocity at different stream-wise position simultaneously. It was found when two actuators act in phase at a forcing frequency St_A of 0.16, the anti-symmetric motion (mode 1) in the wake was suppressed and the periodic changes in the size of the separation bubble (mode 2) were promoted.

Peer-review under responsibility of The Chinese Society of Theoretical and Applied Mechanics (CSTAM).

Keywords: Active flow control; synthetic jet; D-shaped bluff body

Nomenclature

C_μ	momentum ratio of the synthetic jets
H	height of the D-shaped body, m
R_{uu}	correlations of fluctuating velocity
St_A	Strouhal number for the forcing frequency, $f_A H/U$
u	instantaneous stream-wise velocity, m/s
u_n	reconstructed n-th mode stream-wise velocity, m/s
u'	root-mean-square value of stream-wise velocity, m/s
U	free-stream velocity, m/s
x, y, z	spatial coordinates, m
$\Lambda^{(n)}$	eigenvalues of the correlation matrix for $\tau = 0$
$\phi^{(n)}$	eigenvector of the correlation matrix for $\tau = 0$
ρ_{pu}	correlation coefficient between the fluctuating pressure $y = 0$ and velocity
τ	time interval, s

* Corresponding author. Tel.: +86-411-8470-6202 ; fax: +86-411-8470-6202.
E-mail address: gaonan@dlut.edu.cn

Peer-review under responsibility of The Chinese Society of Theoretical and Applied Mechanics (CSTAM).

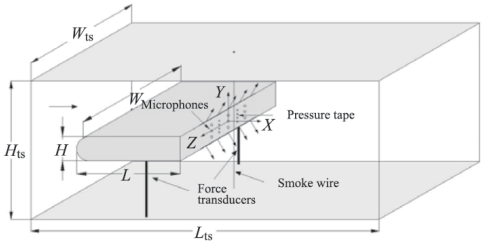

Fig. 1. Schematics of the test rig

1. Introduction

The flow over a D-shaped bluff body separates at the trailing edges and formed large scale wake structures [1,2]. Effectively control of the wake structures can reduce the form drag associated with the flow separations. Pastoor et al. [3] used a pair of synthetic jet actuators to force the wake behind a D-shaped body. The actuator produced periodic jet flows from the upper and the lower edges of the rear surface and the velocity variations of the two actuators were in phase. They found the drag was reduced when the actuation frequency was $0.1 < St_A < 0.2$ but increased when the actuation frequency was $St_A = 0.24$. When the actuation frequency was $St_A = 0.15$ and C_μ was larger than 0.5%, the drag reduced 15% for the flow with a Reynolds number of 47000. Parkin et al. [4] studied the wake using numerical simulation and dynamic mode decomposition (DMD). They found significant drag reduction was observed at $St_A = 0.11$ for momentum ratio of 0.8%. The mean circulation bubble was extended by the symmetric vortices, the base pressure thus increased and drag force reduced.

Li et al. [5] studied the wake behind a D-shaped model similar to that used by [3] but with a smaller forcing strength.They found that when the actuators were in-phased with a C_μ of 0.1% and the actuation frequency was $St_A = 0.16$, the drag reduced 5% for the flow with a Reynolds number of 47000. When the actuators were anti-phased and the actuation frequency was $St_A = 0.24$, the drag increased for about 24%. Li et al. [5] also visualized the flow using a smoke-wire visualization technique. They argued that when the wake was forced in-phased by the two actuators, a pair of symmetric wake structures were produced, these structures postponed the formation of the counter-rotating von-Karman type of wake structures, thus the drag was reduced. The statistical analysis of the wake structures based on a larger number of samples was not performed before. The current investigation focused on the modal decomposition of the instantaneous velocity distribution acquired using a vertically aligned single-wire array. The experimental method will be discussed in the next section, followed by the results and discussions.

2. Experimental methods

The experiments were performed in the same facility (Fig. 1) used by Li et al.[5]. A hotwire array with 14 single hot-wire probe was used to measure the velocity. The wires were positioned with an equal distance of 0.23H between y/H = -1.5 and 1.5 along the cross-flow direction. A tungsten wire of 4.5 microns diameter and approximately 1.2 mm length was used to sensor the flow for each wire. The probes were connected to a 16-channel Hanghua CTA-02A constant temperature anemometry system. An over heat ratio of 1.8 was used for every channel. The signals from the hotwires were offset, low-pass-filtered at a cutoff frequency of 6 kHz, and then sampled at a frequency of 2048Hz using a NI PCI-6014 DAQ card and a Labview routine. The sampling time for each record is 150s. The hot wire probes were calibrated in the wind tunnel with the D-shaped model removed. The resulting response curves were fit with a four-order polynomial, and a modified cosine law.

The instantaneous velocity $u(y,t)$ can be decomposed into 14 modes using Proper Orthogonal Decomposition (POD)

$$u(y,t) = \sum_{n=1}^{14} a_n(t)\phi^{(n)}(y),$$

where the coefficients for mode n were obtained by projecting the velocity $u(y,t)$ onto a set of orthogonal basis

$$a_n(t) = \int_{-1.5H}^{1.5H} u(y,t)\phi^{(n)}dy.$$

The orthogonal basis $\phi^{(n)}$ was obtained by computing the eigenvectors of the correlation matrix

$$\int R(y,y',\tau=0)\phi^{(n)}(y')dy' = \Lambda^{(n)}\phi^{(n)}(y).$$

The motion for the n-th mode can be re-constructed using $a_n(t)$ and $\phi^{(n)}(y)$,

$$u_n(y,t) = a_n(t)\phi^{(n)}(y).$$

3. Results and Discussion

The fluctuating velocity for un-controlled flow (case I), flow with in-phased actuation of $St_A = 0.16$ (case II) and flow with anti-phased actuation of $St_A = 0.24$ (case III) are shown in Fig.2. At $x/H = 2$, there are two maxima in the profile of the fluctuating velocity in cases I and III, while there is only 1 maximum in case II. The pressure-velocity correlations in Fig.3 for $x/H = 2$ also showed that case II was different from cases I and III.

A data block of 0.2 second duration measured at $x/H = 2.0$ was decomposed into different modes using POD. The original velocity trace and the data for modes 1-3 are shown in Fig.4. There area pair of regions with positive and negative fluctuating velocities occurred simultaneously in mode 1 for the three cases suggesting motion of mode 1 was an anti-symmetric von Karman vortex street (see Fig. 6). The motion for mode 2 was caused by the periodic changes in the size of the separation bubble behind the bluff body. The characteristic frequency of mode 2 was twice of that for mode 1 as the structures in the upper and lower row could both caused the bubble size to change. The variances for the original velocity data and those for different modes are shown in Fig.5. Modes 1 and 2 are the two major contributors to the total fluctuations. In case II, the contribution of mode 1 was smaller than it did in the other two cases, the contribution of mode 2 became large, suggesting the in-phased actuation at $St_A = 0.16$ suppressed mode 1 and promoted mode 2, this was also suggested by the reconstructed velocity $u_1(y,t)$ for mode 1 in case II, where von Karman vortices were not as obvious at some occasions, at the same time the fluctuations in mode II became relatively large. More investigations are needed to clarify the competing mechanism between different modes.

4. Conclusions

Wake behind a D-shaped bluff body were studied using a rake of 14 hot-wire probes. The instantaneous velocity downstream of the bluff body at $x/H = 2.0$ and $-1.5 \le y/H \le 1.5$ were sampled simultaneously. It was found when two actuators act in phase at a forcing frequency St_A of 0.16, the anti-symmetric motion (mode 1) in the wake was suppressed and the periodic changes in the size of the separation bubble (mode 2) were promoted, similar to what was postulated by Pastoor et al.[3] and Li et al.[5].

Acknowledgement This work was supported by 973 plan (2014CB744100).

References

[1] P.W. Bearman, Investigation of the flow behind a two-dimensional model with a blunt trailing edge and fitted with splitter plates, J. Fluid Mech. 21 (1965) 241C256.

[2] H. Park, D. Lee, W. Jeon, S. Hahn, J. Kim, J. Kim, J. Choi, Drag reduction in flow over a two-dimensional bluff body with a blunt trailing edge using a new passive device, J. Fluid Mech. 563 (2006) 389C414.

[3] M. Pastoor, L. Henning, B.R. Noack, K. Rudibert, T. Gilead, Feedback shear layer control for bluff body drag reduction, J. Fluid Mech. 608 (2008) 161C196.

[4] Parkin D.J., Thompson M.C. and Sheridan J. 2014 Numerical analysis of bluff body wakes under periodic open-loop control. J. Fluid Mech. 739: 94-123

[5] Y. Li, H. Bai, N. Gao, Drag of a D-shaped bluff body under small amplitude harmonic actuation Theoretical and Applied Mechanics Letters 5 (2015) 35C38

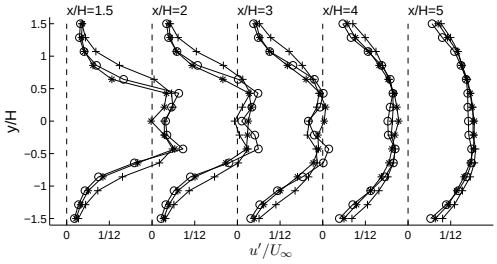

Fig. 2. Distributions of the fluctuating velocity for ∘ case I:un-forced flow, ∗ case II:in-phased forcing at St_A =0.16 and + case III:anti-phased forcing at St_A = 0.24.

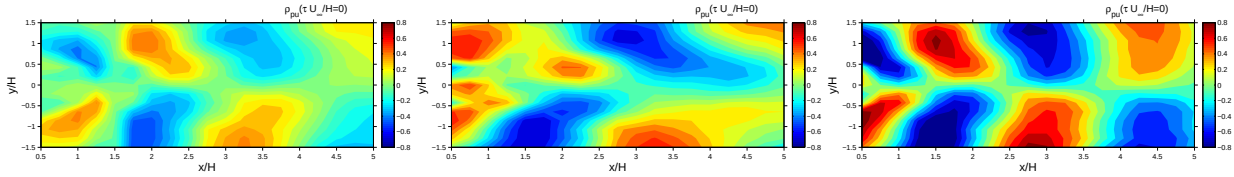

(a) (b) (c)

Fig. 3. Distributions of the correlation coefficient between the fluctuating wall pressure at $y = 0$ and $z = 0$ and the fluctuating velocity at $-1.5 \le y/H \le 1.5$ for (a) case I:un-forced flow, (b) case II:in-phased forcing with St_A =0.16 and (c) case III:anti-phased forcing with St_A = 0.24.

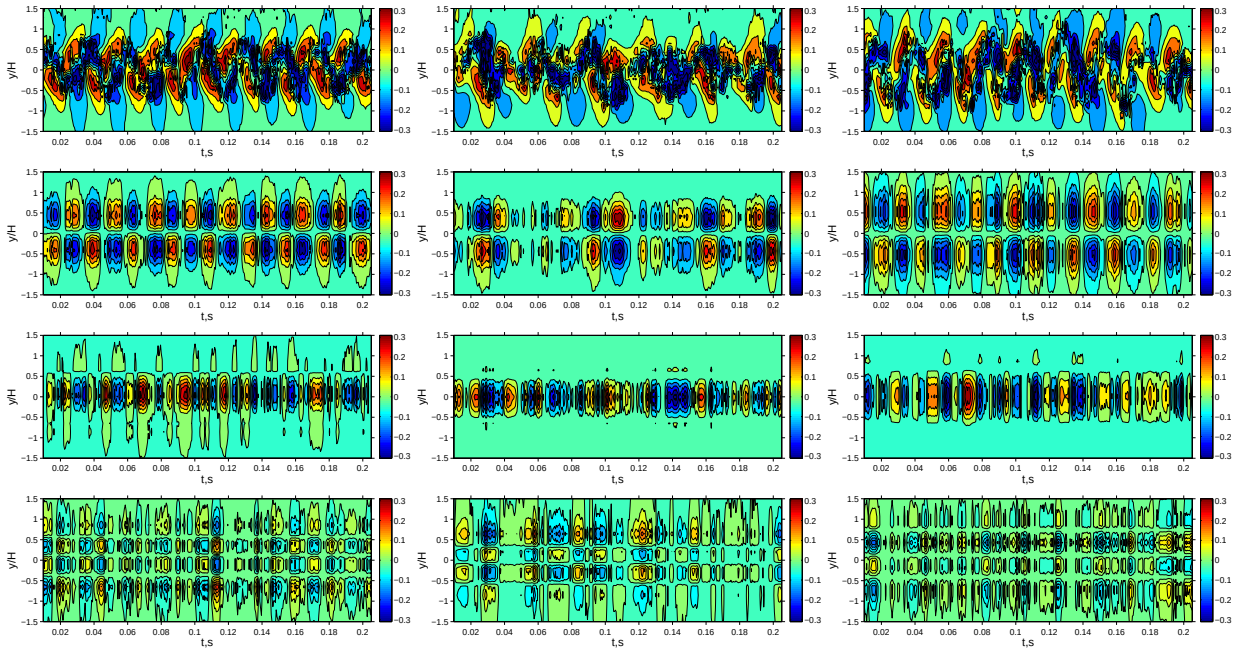

(a) (b) (c)

Fig. 4. Distributions of (from top to bottom) typical instantaneous velocity ($u(y,t)$), re-constructed velocity for mode 1 ($u_1(y,t)$), 2 ($u_2(y,t)$) and 3 ($u_3(y,t)$) at $-1.5 \le y/H \le 1.5$ and $x/H = 2.0$ for (a) case I:un-forced flow, (b) case II:in-phased forcing with St_A =0.16 and (c) case III:anti-phased forcing with St_A = 0.24.

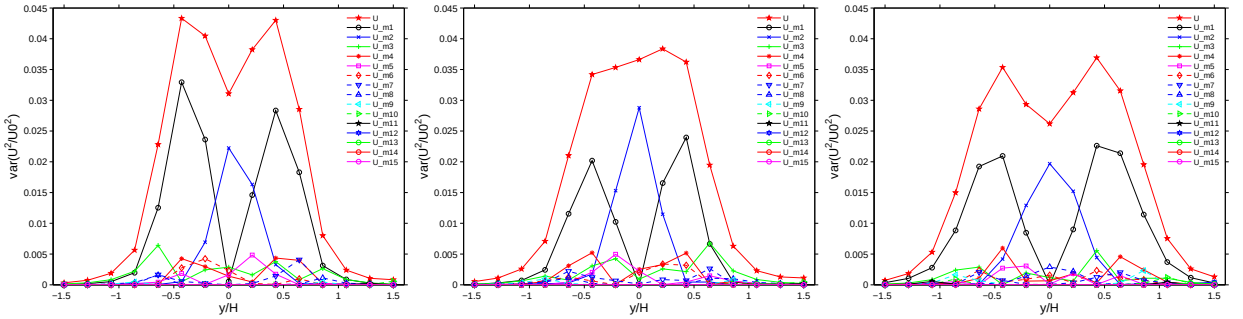

(a) (b) (c)

Fig. 5. Distributions of the variance of the original instantaneous velocity and re-constructed velocity for modes 1 to 14 at $x/H = 2.0$ for (a) case I:un-forced flow, (b) case II:in-phased forcing with St_A =0.16 and (c) case III:anti-phased forcing with $St_A = 0.24$.

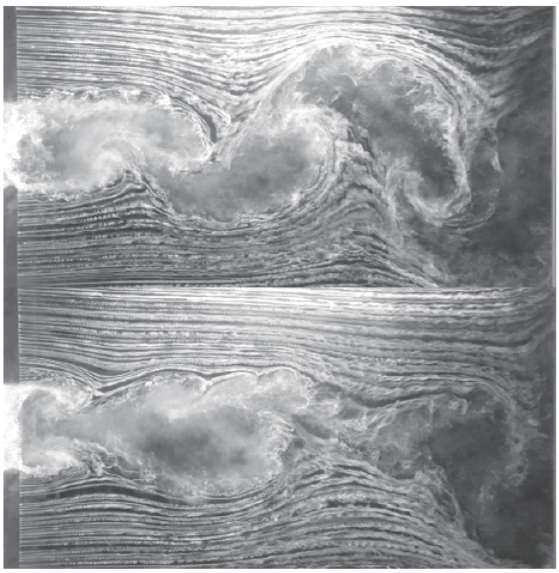

Fig. 6. Smoke-wire visualization for (top) case I:un-forced flow, (bottom) case II:in-phased forcing with St_A =0.16